

# Use of *in vivo* chlorophyll *a* fluorescence to quantify short-term variations in the productive biomass of intertidal microphytobenthos

João Serôdio<sup>1,2,\*</sup>, Jorge Marques da Silva<sup>2,3</sup>, Fernando Catarino<sup>1,2</sup>

<sup>1</sup>Instituto de Oceanografia, <sup>2</sup>Departamento de Biologia Vegetal and <sup>3</sup>Centro de Engenharia Biológica, Faculdade de Ciências da Universidade de Lisboa, Campo Grande, 1749–016 Lisboa, Portugal

**ABSTRACT:** This study investigates the ability to use *in vivo* chlorophyll *a* fluorescence to quantify the productive biomass of undisturbed microphytobenthic communities, defined as the photosynthetic biomass present in the photic zone of the sediment and actually contributing to measurable photosynthesis. The purposes of defining and quantifying productive biomass are (1) to evaluate the effect of the migratory rhythms on the variability of microphytobenthic photosynthesis and (2) to characterise the community photophysiological response independently of the migratory stage, through the estimation of biomass-specific, community-level photosynthetic rates. The possibility of using chl *a* fluorescence, as measured non-destructively at the sediment surface, to trace variations in the productive biomass of microphytobenthos was confirmed by testing (1) the variability of the relationship between fluorescence emission and chl *a* concentration under varying temperature and irradiance levels and (2) the effects of natural variability in the vertical profile of chl *a* within the photic zone of the sediment on the depth-integrated fluorescence signal,  $F$ , measurable at the surface. Dark-level fluorescence,  $F_0$ , was found to allow for tracing variations in chl *a* concentration under the range of temperature and irradiance variability found *in situ*. Depth-integration of fluorescence emission resulted in only a fraction of total productive biomass being detectable at the surface. However, this fraction was found to be sufficiently constant to allow for the use of  $F_0$  to proportionally follow variations in community productive biomass. On average, measurements of productive biomass on natural samples overestimated by a factor of 1.30 during low tide and underestimated by a factor of 0.66 during high tide, mostly due to variations in the chl *a* profile in the photic zone associated with vertical migrations. The method was applied to intertidal microphytobenthic communities of the Tagus estuary, Portugal, by non-destructively measuring  $F_0$  (using pulse amplitude modulated fluorometry) and photosynthesis (using oxygen microelectrodes) on the same samples under *in situ* conditions. The results showed that a significant proportion of the hourly and fortnightly variability in the community photosynthetic light response was explained solely by variations in  $F_0$  associated with movements of microalgae, identifying migratory rhythms as the main cause for short-term variability in intertidal benthic primary productivity.

**KEY WORDS:** Microphytobenthos · Photosynthesis · Migratory rhythms · Chlorophyll *a* fluorescence · Light absorption

Resale or republication not permitted without written consent of the publisher

## INTRODUCTION

The efficiency of utilisation of sunlight by photosynthetic communities is determined by the ratio of photo-

synthetically converted to available light energy (Morel 1978, Dubinsky et al. 1984). Because photosynthetic production results from the sequential absorption of light and conversion of the absorbed light energy, the community-level photosynthetic efficiency is determined both by the efficiency of light absorption (the ratio of absorbed to available light) and by the efficiency of conversion of absorbed light (the ratio of converted to

\*Present address: Departamento de Biologia, Universidade de Aveiro, Campus de Santiago 3810-193 Aveiro, Portugal. E-mail: jserodio@bio.ua.pt

absorbed light). Intertidal microphytobenthos living on soft-sediment habitats is composed of motile microalgae exhibiting rhythmic vertical migrations across the photic zone of the sediment in close synchronisation with tidal and day/night cycles (Round & Palmer 1966, Paterson 1986). The vertical movement of the cells results in rapid and substantial variations of the fraction of the incident light on the surface that is intercepted by the microalgal light-harvesting complexes and absorbed for photosynthesis. Variability in the community primary production may thus originate not only from changes in the quantum efficiency of photosynthesis, determined by the photophysiological characteristics of the microalgal population exposed to light, but also from variations in light absorption efficiency.

The quantification of the fraction of incident light that is absorbed for photosynthesis by the whole microphytobenthic community is necessary to distinguish the contribution of migratory rhythms and photophysiological processes for the short-term variability often observed in the community photosynthesis. By eliminating the variability associated with light absorption, this also allows characterisation of the photophysiological response of the benthic microalgae independent of variations in cell concentration in the photic zone. This has been approached by the calculation of areal biomass-specific primary production rates, through the normalisation to the chlorophyll (chl) *a* content of the upper millimetres of sediment (Pinckney & Zingmark 1991, Blanchard & Montagna 1992, Brotas & Catarino 1995). However, in spite of its widespread utilisation, this practice has some important shortcomings. First, because the sectioning depth is much larger than the photic zone of the sediment, most of the quantified biomass is certainly not contributing to the measured production (Grant 1986, Pinckney & Zingmark 1993). This makes it impossible to distinguish changes in the biomass present in the photic zone from physiological processes such as photoadaptation or photoinhibition. Second, biomass-specific photophysiological parameters calculated in this way are not directly comparable with biomass-specific values obtained either for resuspended microphytobenthos or phytoplankton, for which it may be assumed that all quantified chl *a* contributes equally to measured photosynthesis. Third, it is a destructive method, which prevents repeated measurements on the same sample over time and limits the precision and the spatial and temporal resolution of the experiments.

This study addresses the definition and measurement of the productive biomass of microphytobenthic assemblages, a quantity defined on the basis of the photosynthetic biomass present in the photic zone of the sediment, and allowing the normalisation of photosynthetic rates to the chl *a* actually contributing to measured photosynthesis. The study examines the

possibility of utilising *in vivo* chl *a* fluorescence, as measured non-destructively near the sediment surface using a pulse amplitude modulation (PAM; Schreiber et al. 1986) fluorometer to (1) monitor variations in the productive biomass of undisturbed microphytobenthic assemblages and (2) estimate biomass-specific community-level photosynthetic rates and photosynthesis-irradiance (*P* vs *E*) curve parameters. Non-intrusive measurement of fluorescence intensity at the sediment surface was previously seen to allow the tracing of migratory rhythms, through the detection of variations in the chl *a* content of the upper layers of the sediment (Serôdio et al. 1997), but the relation between the measured fluorescence signal and productive biomass was not determined.

The method was applied in the quantification of the effects of changes in productive biomass in the photosynthetic light response of microphytobenthos communities of the Tagus estuary, Portugal, under *in situ* conditions, over hourly (migratory rhythms), fortnightly and seasonal time scales. The basis for the method is first established by considering the theoretical relationship between photosynthesis and productive biomass of microphytobenthic assemblages, and the depth-integrated emission of chl *a* fluorescence, measurable at the sediment surface.

## THEORY

**Community-level photosynthesis and productive biomass.** The rate of photosynthesis taking place in a unit volume of sediment at depth *z* is determined by the light available at that depth, the fraction of this light which is absorbed by the energy-absorbing pigments of the light-harvesting complexes of the photosystems, and the efficiency of photosynthetic conversion of absorbed light (Kiefer et al. 1989, Kolber & Falkowski 1993):

$$P(z) = E_0(z)a^*_{\text{PAR}}(z)c(z)\phi P(z) \quad (1)$$

where  $E_0$  is the incident scalar irradiance, integrated over the spectrum of photosynthetically active radiation (PAR; 400 to 700 nm),  $a^*_{\text{PAR}}$  is the optical spectrally averaged absorption cross-section of energy-absorbing pigments normalised to chl *a* [assuming  $E_0a^*_{\text{PAR}} = \int_{\text{PAR}} E_0(\lambda)a^*(\lambda)d\lambda$ ],  $c$  is the chl *a* concentration, and  $\phi P$  is the quantum yield of photosynthesis (see Table 1 for notation); the product of  $a^*_{\text{PAR}}$  and  $c$  defines the efficiency of photosynthetic light absorption at depth *z*, determined by the ratio of available to absorbed irradiance. The photosynthetic rate of the microphytobenthic community is given by integrating over depth the rate of photosynthesis at each depth *z* between the surface and some depth  $z = z_p$ , at which the rate of photo-

Table 1. Notation used in the text

$a^*_{\text{PAR}}, a^*_{650}$	Optical spectral (400 to 700 nm, 650 nm) absorption cross-section normalised to chl <i>a</i> ( $\text{m}^2 \text{mg}^{-1} \text{chl } a$ )
$\alpha, \alpha^{\text{B}}$	Initial slope and biomass-specific initial slope of the depth-integrated <i>P</i> vs <i>E</i> curve [ $\text{mmol O}_2 \text{m}^{-2} \text{h}^{-1}(\mu\text{mol m}^{-2} \text{s}^{-1})^{-1}$ , $\text{mmol O}_2 \text{mg}^{-1} \text{chl } a \text{h}^{-1}(\mu\text{mol m}^{-2} \text{s}^{-1})^{-1}$ ]
<i>c</i>	Chl <i>a</i> concentration ( $\text{mg chl } a \text{m}^{-3}$ )
$c_{\text{P}}, c_{\text{F}}$	Productive biomass and biomass detected by depth-integrated fluorescence ( $\text{mg chl } a \text{m}^{-2}$ )
chl	Chlorophyll
$E, E_{650}$	Downwelling spectral irradiance (400 to 700 nm, 650 nm) at the sediment surface ( $\text{W m}^{-2} \text{nm}^{-1}$ or $\mu\text{mol m}^{-2} \text{s}^{-1}$ )
$E_0$	Scalar spectrally averaged (400 to 700 nm) irradiance ( $\text{W m}^{-2} \text{nm}^{-1}$ or $\mu\text{mol m}^{-2} \text{s}^{-1}$ )
$\epsilon$	Community-level efficiency of photosynthetic light absorption
<i>F</i>	Depth-integrated upwelling fluorescence intensity detected at the surface (V)
$F(z)$	Upwelling fluorescence intensity emitted at depth <i>z</i> ( $\text{W m}^{-2}$ or $\mu\text{mol m}^{-2} \text{s}^{-1}$ )
$F_0, F_{\text{m}}$	Dark-level and maximum fluorescence intensity emitted by a dark-adapted sample (V)
$F_{\text{ss}}, F'_{\text{m}}$	Steady-state and maximum fluorescence intensity emitted by a light-adapted sample (V)
<i>f</i>	Fraction of productive biomass detected by depth-integrated fluorescence
$\phi F$	Quantum yield of fluorescence [quanta emitted (quanta absorbed) $^{-1}$ ]
$\phi F_0, \phi F_{\text{m}}$	Dark-level and maximum quantum yield of chl <i>a</i> fluorescence of a dark-adapted sample [quanta emitted (quanta absorbed) $^{-1}$ ]
$\phi P$	Quantum yield of photosynthesis [mol O <sub>2</sub> (mol quanta absorbed) $^{-1}$ ]
<i>G</i>	Conversion factor between detected fluorescent irradiance and fluorometer output ( $\text{V W}^{-1} \text{m}^2$ )
$k_{650}, k_{710}, k_{\text{F}}$	Attenuation coefficients for downwelling exciting irradiance and upwelling fluorescent irradiance; $k_{\text{F}} = k_{650} + k_{710}$ ( $\text{mm}^{-1}$ )
$k_{\text{P}}$	Attenuation coefficient for downwelling photosynthetically active irradiance ( $\text{mm}^{-1}$ )
$L_{\text{F}}, L_{\text{P}}$	Detection limits for fluorescence intensity (V) and photosynthetic rate ( $\text{mmol O}_2 \text{dm}^{-3} \text{h}^{-1}$ )
<i>m</i>	Convexity of the <i>P</i> vs <i>E</i> curve
$\mu_{\text{PAR}}, \mu_{650}$	Average cosine (mean cosine of the average path direction of incident photons)
$P, P^{\text{B}}$	Depth-integrated and depth-integrated biomass-specific rate of gross photosynthesis ( $\text{mmol O}_2 \text{m}^{-2} \text{h}^{-1}$ , $\text{mmol O}_2 \text{mg}^{-1} \text{chl } a \text{h}^{-1}$ )
$P(z)$	Gross photosynthetic rate at depth <i>z</i> ( $\mu\text{mol O}_2 \text{dm}^{-3} \text{h}^{-1}$ )
$P_{\text{m}}, P_{\text{m}}^{\text{B}}$	Depth-integrated and depth-integrated biomass-specific maximum rate of gross photosynthesis ( $\text{mmol O}_2 \text{m}^{-2} \text{h}^{-1}$ , $\text{mmol O}_2 \text{mg}^{-1} \text{chl } a \text{h}^{-1}$ )
PAR	Photosynthetically active radiation, 400 to 700 nm ( $\mu\text{mol m}^{-2} \text{s}^{-1}$ )
$R_{\text{PAR}}, R_{650}$	Irradiance reflectance (ratio of upward to downward irradiance)
<i>z</i>	Depth below the sediment surface (mm)
$z_{\text{F}}$	Depth at which fluorescence intensity measured at the surface equals $L_{\text{F}}$ (mm)
$z_{\text{P}}$	Depth at which gross rate of photosynthesis equals $L_{\text{P}}$ (mm)

synthesis equals  $L_{\text{P}}$ , the minimum detectable value with the measuring method in use. Depth-integrated photosynthesis may be expressed as a function of the downwelling irradiance at the surface of the sediment, *E*, the parameter routinely measured when characterising light availability for benthic communities (Grant 1986, Pinckney & Zingmark 1993, Brotas & Catarino 1995), by:

$$P(E) = \int_0^{z_{\text{P}}} P(z) dz \quad (2)$$

$$= \int_0^{z_{\text{P}}} E a^*_{\text{PAR}}(z) c(z) \phi P(z) \frac{1 - R_{\text{PAR}}(z)}{\mu_{\text{PAR}}(z)} e^{-k_{\text{P}}z} dz$$

where  $R_{\text{PAR}}$  is the irradiance reflectance (the ratio of upward to downward irradiance),  $\mu_{\text{PAR}}$  the average cosine (the mean cosine of the average path direction of incident photons), and  $k_{\text{P}}$  the attenuation coefficient for downwelling photosynthetically active irradiance within the sediment (Kühl & Jørgensen 1994).

The community-level microphytobenthic photosynthesis is thus determined by the joint vertical distribution of the fraction of light entering the sediment that is

absorbed for photosynthesis and of the quantum yield of photosynthesis along the gradient of available light. Migratory rhythms affect community-level photosynthetic rates by altering the fraction of the light incident at the surface that is absorbed for photosynthesis by the whole community, caused by changes in the amount of chl *a* in the photic zone of the sediment. It is therefore useful to define the productive biomass of the microphytobenthic assemblage as the total chl *a* present in the photic zone, weighted at each depth by its contribution to total photosynthesis, given by the fraction of incident irradiance that is available for photosynthesis (Fig. 1A):

$$c_{\text{P}} = \int_0^{z_{\text{P}}} c(z) \frac{1 - R_{\text{PAR}}(z)}{\mu_{\text{PAR}}(z)} e^{-k_{\text{P}}z} dz \quad (3)$$

Defined in these terms,  $c_{\text{P}}$  has units of milligrams of chl *a* per square metre and enables the normalisation of community-level photosynthetic rates ( $\text{mmol O}_2 \text{m}^{-2} \text{h}^{-1}$ ) to yield areal biomass-specific rates,  $P^{\text{B}}$  ( $\text{mmol O}_2 \text{mg}^{-1} \text{chl } a \text{h}^{-1}$ ), thus eliminating the effect of changes

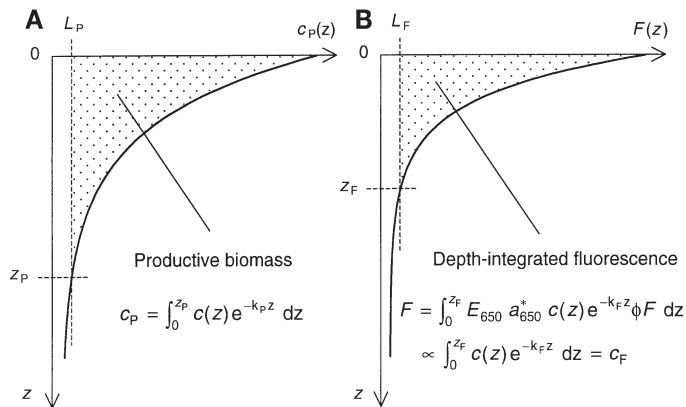


Fig. 1. (A) Productive biomass,  $c_p$ , and (B) depth-integrated fluorescence,  $F$  (shaded areas), defined by detection limits  $L_p$  and  $L_F$ , which determine  $z_p$  and  $z_F$  (Eqs 7 & 8). For clarity, curves correspond to homogeneous chl  $a$  profiles, and parameters  $R$  and  $\mu$  are not included in equations

in biomass on community photosynthesis. To normalise to  $c_p$  has the advantage of not attributing the same weight to all chl  $a$  present in some section of the sediment, in spite of the certainty that not all the quantified chl  $a$  equally contributes to measured photosynthesis (Grant 1986, Pinckney & Zingmark 1993).

**Depth-integrated fluorescence and tracing of productive biomass.** As with photosynthesis, the emission of chl  $a$  fluorescence may be described by the product of the rate of light absorption and the quantum efficiency of the conversion of absorbed light into fluorescence (Falkowski & Kiefer 1985, Büchel & Wilhelm 1993). The fluorescence emitted at any depth  $z$ ,  $F(z)$ , is given by the product of the exciting irradiance applied by the fluorometer (in the case of the used PAM fluorometer, a narrow-band red light beam of measuring light peaking at  $\lambda = 650$  nm) available at that depth, the fraction of this irradiance that is absorbed by the PSII light-harvesting complex, and the quantum yield of fluorescence, integrated over the range of detectable wavelengths (with the PAM fluorometer,  $\lambda > 710$  nm):

$$F(z) = E_{650} a_{650}^*(z) c(z) \phi F(z) \frac{1 - R_{650}(z)}{\mu_{650}(z)} e^{-k_{650}z} \quad (4)$$

where  $k_{650}$  is the attenuation coefficient for downwelling exciting irradiance. The fluorescence signal measured non-invasively at the surface of the sediment represents the integration over depth of the upwelling fluorescence emitted at each depth  $z$  that is detectable at the surface:

$$F = \int_0^{z_F} F(z) e^{-k_{710}z} dz G \quad (5)$$

where  $z_F$  is the depth at which the fluorescence detected at the surface equals  $L_F$ , the minimum detectable intensity,  $k_{710}$  is the attenuation coefficient

for the upwelling fluorescent irradiance, and  $G$  is a constant representing the conversion between fluorescence and instrument output (Fig. 1B) (for simplicity, the attenuation of the exciting light and of the emitted fluorescence in the air, and the reflexion losses at the sediment-air or sediment-water interface are assumed to be constants and are not parameterised).

The rationale for the use of chl  $a$  fluorescence to trace variations in productive biomass is based on the fact that any changes in chl  $a$  in the photic zone causing variations in  $c_p$  will concurrently cause proportional variations in the intensity of fluorescence emission,  $F$  (Kiefer et al. 1989, Chamberlin et al. 1990). The applicability of the method depends on a number of factors that potentially affect the proportionality between fluorescence emission and chl  $a$  concentration, namely the photophysiological relationship between the 2 variables and their relative vertical distribution within the photic zone of the sediment.

**Fluorescence versus chl  $a$  concentration:** Regarding the relationship between fluorescence emission and chl  $a$  concentration at each depth  $z$  (i.e. not depth-integrated), the variability in  $E_{650}$ ,  $a_{650}^*$  and  $\phi F$  (Eq. 4) over the range of natural environmental conditions and migratory stages has to be sufficiently low to not confound the effects of variations in chl  $a$  on  $F$  ( $k_{650}$ ,  $R_{650}$  and  $\mu_{650}$  are determined by the optical characteristics of the sediment).  $\phi F$ , being directly affected by the functioning of the photosynthetic apparatus, is the main cause for large changes in the intensity of fluorescence on short time scales (Falkowski & Kiefer 1985, Krause & Weis 1991). As the intertidal environment is characterised by high variability in light and temperature levels (Serôdio & Catarino 1999), both factors that primarily affect  $\phi F$ , large variability in fluorescence emission due to variations in  $\phi F$  are to be expected.  $\phi F$  varies between 2 extreme values, the minimum- or dark-level quantum yield of fluorescence,  $\phi F_0$ , and the maximum quantum yield of fluorescence,  $\phi F_m$  (corresponding to fluorescence intensities  $F_0$  and  $F_m$ ,  $F_s$  denoting the intermediate emission of a light-adapted sample).

**Depth-integrated fluorescence:** Even under the conditions for the existence of a linear relationship between fluorescence emission and chl  $a$  concentration at each depth  $z$ , depth-integration may cause  $F$  and  $c_p$  to vary disproportionately. First, due to the attenuation of upwelling fluorescence,  $F$  may detect only a fraction of total  $c_p$ , meaning that deeper zones of the sediment may contain chl  $a$  and be exposed to irradiance levels high enough to drive photosynthesis while not contributing to the fluorescence signal measured at the surface. The upwelling attenuation of fluorescence causes the proportion between  $F(z)$  and  $c(z)$  to vary with depth, and the relationship between depth-inte-

grated  $F$  and  $c_p$  to become affected by the shape of the chl  $a$  profile over the depth interval defined by  $z_p$ . Therefore, a condition under which  $F$  remains proportional to  $c_p$  is when the chl  $a$  profile over the photic zone does not change over the migratory cycles, that is, the migratory movements affect mostly the total chl  $a$  content of the photic zone but not significantly its vertical distribution. Second, the relation between  $F$  and  $c_p$  may further vary with  $E$  and  $c$  due to uncorrelated variations in  $z_p$  (expected to increase with  $E$ ) and  $z_F$  (dependent on the non-linear response of  $\phi F$  to changes in  $E$ ). As can be deduced for the simplest case of a uniform chl  $a$  profile in the photic zone, variations in the fraction of total productive biomass detected by depth-integrated fluorescence,  $f$ , given by the ratio between  $c_F$ , the biomass detected by  $F$ , and  $c_p$  (considering that  $R_{650}/R_{PAR}$  and  $\mu_{650}/\mu_{PAR}$  remain relatively invariant and close to 1, and defining  $k_F = k_{650} + k_{710}$ ),

$$f = \frac{c_F}{c_p} = \frac{\int_0^{z_F} c e^{-k_F z} dz}{\int_0^{z_p} c e^{-k_p z} dz} = \frac{k_p}{k_F} \left( \frac{1 - e^{-k_F z_F}}{1 - e^{-k_p z_p}} \right) \quad (6)$$

may occur through changes in  $z_p$  and  $z_F$ , as they are dependent on  $E$  and  $c$ :

$$z_p = \frac{1}{-k_p} \ln \left[ \frac{L_p}{E a^*_{PAR} c \phi P} \left( \frac{1 - R_{PAR}}{\mu_{PAR}} \right)^{-1} \right] \quad (7)$$

$$z_F = \frac{1}{-k_F} \ln \left[ \frac{L_F}{E_{650} a^*_{650} c \phi F} \left( \frac{1 - R_{650}}{\mu_{650}} \right)^{-1} \right] \quad (8)$$

However, the effects of varying  $E$  or  $c$  on  $f$  variability depend on the detection limits  $L_F$  and  $L_p$ : if these are sufficiently low, then  $e^{-k_p z_p} \approx 0$  and  $e^{-k_F z_F} \approx 0$  (Eq. 6), and  $f$  becomes independent of the chl  $a$  profile and of  $E$ , ensuring that  $F$  proportionally follows the variations in  $c_p$ .

The ability of depth-integrated chl  $a$  fluorescence to trace variations in the productive biomass of microphytobenthic communities was approached by testing the conditions for the verification of a linear relationship between  $F$  and  $c_p$ : (1) the invariability of the relationship between fluorescence emission and chl  $a$  concentration under varying temperature and light levels, and (2) the invariability of  $f$  over variations in  $E$  or  $c$ , and over variations in the depth profile of chl  $a$  in natural samples under the range of *in situ* conditions.

## METHODS

**Measurement of chl  $a$  fluorescence and photosynthesis.** Chl  $a$  fluorescence was measured using a PAM fluorometer (PAM 101 chlorophyll fluorometer, Heinz Walz, Germany) and recorded on a strip chart recorder. Fluorescence emission was induced by weak modu-

lated red light (ca  $0.1 \mu\text{mol m}^{-2} \text{s}^{-1}$ , 650 nm), emitted at a frequency of 1.6 kHz when measuring  $F_0$ , or 100 kHz when measuring other parameters.  $F_0$  was measured applying the highest possible intensity of exciting beam, not inducing any significant variable fluorescence, and maximum instrument damping to maximise the signal to noise ratio.  $F_0$  readings were considered after signal stabilisation following sample darkening. Actinic and saturating light was provided by an FL-101 fibre illuminator (Schott KL1500 halogen lamp, Schott, Germany).

Photosynthesis was measured using Clark-type oxygen microelectrodes (5 to 20  $\mu\text{m}$  tip 737-GC, Diamond General, USA) according to Revsbech & Jørgensen (1983). The microelectrode was positioned vertically within the sediment using a micromanipulator (MM33, Diamond General) and was connected to a picoammeter (Model 8100 Electrometer, Keithley Instruments, USA). Illumination was provided by the same light source and fiberoptics used for measuring chl  $a$  fluorescence. Irradiance incident at the surface of the sediment was measured by positioning a PAR quantum sensor (LI-192SB, Li-Cor, USA) at the level of sediment surface.

**$F$  versus  $c$ : temperature and light effects.** The variability of the relationship between fluorescence intensity and chl  $a$  concentration was tested by measuring fluorescence emission ( $F_0$ ,  $F_m$ ,  $F_s$ , and  $F_m'$ , the maximum fluorescence level emitted from a light-adapted sample) under the range of *in situ* temperature and irradiance variability, on species representative of the main groups of microalgae occurring in the estuarine microphytobenthos. Although the  $F_0$  emission per unit chl  $a$  is known to be virtually invariable under a wide range of temperature and light intensity conditions, both in higher plants (Schreiber & Bilger 1987, Krause & Weis 1991) and in microalgae (Ting & Owens 1994, Seródio et al. 1997), its measurement requires the dark-adaptation of the sample, which may interfere with the microalgae's behaviour and lead to artifactual migratory responses. Another potential advantage of the use of parameters other than  $F_0$  is the enhanced signal to noise ratio obtained at the higher frequency of measuring light used under actinic or saturating light.

The effects of temperature and irradiance on the parameters  $F_0$ ,  $F_m$ ,  $F_s$ , and  $F_m'$  were studied in the diatom *Phaeodactylum tricornutum* (Böhlin) (culture collection of the IPIMAR - Instituto Português de Investigação Marítima, Lisbon, Portugal), the cyanobacterium *Spirulina maxima* (Setch. et Gard.) (UTEX LB2342), and the euglenophyte *Euglena granulata* (Strain 921, culture collection of the Department of Botany, University of Coimbra, Coimbra, Portugal). These were grown in semi-continuous batch cultures at 20°C under  $50 \mu\text{mol m}^{-2} \text{s}^{-1}$  in a 14 h light:10 h dark cycle as described by Seródio et al. (1997). Fluorescence of

microalgal cultures was measured in a Hansatech DW2 oxygen and fluorescence chamber (Hansatech, UK), coupled to a magnetic stirrer to ensure homogenisation of the algal suspension. Temperature of the sample was controlled by a waterbath (Haake NK22, Haake, Germany). Cells were harvested by centrifugation ( $1000 \times g$ , 5 min) during the exponential growth phase, at room temperature, and were resuspended in fresh growth medium supplemented with  $\text{NaHCO}_3$  (10 mM final concentration).

Temperature effects on fluorescence emission were tested by measuring each fluorescence parameter at 7 different temperatures, from 5 to 35°C, under  $200 \mu\text{mol m}^{-2} \text{s}^{-1}$ . Measurements were made after stabilisation of  $F_0$  at each temperature (minimum 20 min). Three replicate samples were used at each temperature. Temperature was measured in the water circulating around the sample with a temperature sensor (BT1, Delta-T Devices, UK) inserted in the Hansatech DW2 chamber through one of its lateral ports, and connected to a data logger (Delta-T Logger, Delta-T Devices). The values obtained for  $F_m$ ,  $F_s$  and  $F_m'$  were normalised to  $F_0$  measured at growth temperature (20°C).

Light effects on chl *a* fluorescence parameters were tested by measuring the intensity of each type of fluorescence emission under 6 different irradiance levels, ranging from 200 to 2200  $\mu\text{mol m}^{-2} \text{s}^{-1}$ , at 20°C. Three replicate samples were measured at each irradiance. To simulate the application of the technique on microphytobenthos samples under *in situ* conditions, in which the sample darkening must be minimal to avoid potential effects on the migratory rhythm,  $F_0$  and  $F_m$  were measured after a 5 min period of darkness following light exposure. To eliminate the variability caused by differences in the chl *a* content among samples,  $F_s$ ,  $F_m'$  and  $F_m$  were normalised to the value of  $F_0$  measured on the same sample prior to light exposure.

***f* variability with *E* and *c*.** The variability in *f* resulting from changes in *E* and *c* (not considering changes in the vertical structure of the photic zone) was evaluated by calculating *f* for the range of variation in *E* and *c* found under natural conditions, by measuring the terms of Eq. (6), which can be rewritten as:

$$f = \frac{k_p}{k_F} \left(1 - \frac{L_F}{F(0)}\right) \left(1 - \frac{L_p}{P(0)}\right)^{-1} \quad (9)$$

where  $P(0)$  and  $F(0)$  are given by considering  $z = 0$  in Eqs (2) & (4), respectively. The terms  $P(0)$ ,  $k_p$ ,  $F(0)$  and  $k_F$  were experimentally determined on vertically homogeneous sediment deposits, prepared by adding microalgae to sediment from which chl *a* was previously removed (Seródio et al. 1997). Sediment without chl *a* was obtained through sterilisation by heat (120°C, 48 h) of natural samples, collected in tidal flats of the Tagus estuary (see below), and the absence of chl *a* was con-

firmed spectrophotometrically. Because of the large quantity of microalgae required for all the experiments, the collection of cells from natural samples was impracticable and microalgae grown in culture were used. The diatom *Phaeodactylum tricornutum* was selected for having dimensions similar to most benthic diatoms and for being non-motile, thus preventing variations in the chl *a* content in the photic zone during the measurements. Cells were harvested by filtering through GF/C Whatman filters, gently scraped from the filter, and mixed with sediment and growth medium (natural seawater enriched with *f/2* nutrients) to obtain a final water content of ca 50% (w/w), which was similar to natural samples and prevented the formation of a heterogeneous vertical distribution of chl *a* during settling. The final cell concentration was set to correspond to the chl *a* concentration within the range of variation observed with natural samples.

$P(0)$  and  $k_p$  were estimated from vertical profiles of photosynthesis within the uniform deposits of sediment and microalgae, by fitting to profiles of  $P(z)/E$  the equation:

$$\ln\left(\frac{P(z)}{E}\right) = \ln\left(\frac{P(0)}{E}\right) - k_p z \quad (10)$$

Photosynthesis was measured at depth intervals of 40  $\mu\text{m}$ , under surface irradiance levels ranging from 30 up to 2300  $\mu\text{mol m}^{-2} \text{s}^{-1}$ . Three independent measurements were made at each depth.  $k_p$  was estimated using the log-linear part of the profiles of photosynthesis corresponding to light-limitation, to optimise the fit of Eq. (10).

$F(0)$  and  $k_F$  were estimated by considering the variation with depth of  $F_0$  emitted from a vertically homogeneous microphytobenthic assemblage, given, from Eqs (4) & (5), by:

$$\int_0^z F(z) e^{-k_{710} z} dz = F(0) \frac{1 - e^{-k_F z}}{k_F} \quad (11)$$

$F_0$  was measured in sediment deposits with different depth but with the same chl *a* concentration, and  $F(0)$  and  $k_F$  were estimated through fitting of Eq. (11) using a quasi-Newton iterative estimation procedure. The sediment and microalgae were deposited in a settling chamber, and chl *a* fluorescence was measured by placing the settling chamber, with transparent bottom, directly on top of the PAM fiberoptics. The depth of each deposit was estimated from its weight, applying a previously established calibration curve relating deposit thickness and weight. The thickness of the deposits used for constructing the calibration curve was determined by reading on the micromanipulator scale the difference between the vertical position of the tip of a microelectrode touching the bottom of the empty settling chamber and touching the surface of the sedi-

ment deposit. The position of the electrode tip was determined by observation through a binocular dissecting microscope. The contribution of background fluorescence emitted by the sediment particles was estimated by measuring  $F_0$  on sediment without chl *a* and was subtracted from the  $F_0$  readings.  $L_F$  and  $L_P$  were estimated by determining the minimum detectable chl *a* fluorescence intensity and rate of photosynthesis under the applied instrumentation settings.  $f$  was calculated for  $E$  values varying up to  $2000 \mu\text{mol m}^{-2} \text{s}^{-1}$ , and for  $c$  values varying from 25 up to  $150 \text{ g chl a m}^{-3}$ , values obtained from  $F_0$  data measured in natural samples in the Tagus estuary.

***f* variability in situ.** The variability in  $f$  in undisturbed samples under natural conditions was characterised by estimating its value for the range of vertical chl *a* profiles in the photic zone occurring under *in situ* conditions. Considering their importance in determining the value of  $f$ , chl *a* profiles were tested for linearity, a condition that ensures proportionality between  $F$  and  $c_p$ .

**Vertical chl *a* profiles in the photic zone:** Under irradiance levels correspondent to the linear part of the  $P$  versus  $E$  curve, the quantum yield of photosynthesis is maximum and constant ( $\phi P = \phi P_m$ ), and, at any depth  $z$ ,  $P(z)$  is expected to be proportional to  $c(z)$  (Eq. 1). In the case of a homogeneous photic zone (depth constants  $a^*$ ,  $c$ ,  $R$  and  $\mu$ ),  $P(z)$  is expected to vary exponentially with  $z$ , and the uniformity of the vertical distribution of chl *a* in the photic zone may be assessed in natural samples by testing the log-linearity of the vertical profiles of  $P(z)/E$  (Eq. 10). Vertical profiles of light-limited photosynthesis measured for the construction of community  $P$  versus  $E$  curves on natural samples under *in situ* conditions (see below) were used to study the shape and variability of the chl *a* profile over migratory cycles. Eq. (10) was fitted by linear regression to vertical profiles of mean  $P(z)$  values calculated by averaging the rates measured under different limiting irradiance levels at each depth.

***f* estimation:** Using the values estimated for  $k_p$  and  $k_F$ ,  $f$  was calculated by applying Eq. (6) and the rationale behind Eq. (10) to vertical profiles of light-limited photosynthesis:

$$f = \frac{\sum_z c(z)e^{-k_F z}}{\sum_z c(z)e^{-k_P z}} = \frac{\sum_z \left( \frac{P(z)}{E} e^{-k_F z} \right)}{\sum_z \left( \frac{P(z)}{E} \right)} \quad (12)$$

**Effects of varying productive biomass on photosynthetic light response.** The method was applied to characterise the variability of  $c_p$  *in situ*, and to assess the quantitative effects of short-term changes in productive biomass on the community photosynthetic light response. Depth-integrated fluorescence and commu-

nity-level  $P$  versus  $E$  curve parameters  $\alpha$  [initial slope,  $\text{mmol O}_2 \text{ m}^{-2} \text{ h}^{-1} (\mu\text{mol m}^{-2} \text{ s}^{-1})^{-1}$ ] and  $P_m$  ( $\text{mmol O}_2 \text{ m}^{-2} \text{ h}^{-1}$ , maximum photosynthesis) were measured on undisturbed natural microphytobenthos samples under the range of conditions found in the estuarine intertidal environment, over hourly, fortnightly and seasonal time scales.

The data thus obtained were also used to further test the applicability of the method over the range of *in situ* conditions, based on the following rationale: under light limitation, on the linear part of the  $P$  versus  $E$  curve,  $\phi P$  is constant, and, in the presence of a vertically homogeneous photic zone,  $\alpha$  may be expected to be linearly related to  $c_p$  (from Eq. 2):

$$\alpha = \frac{P}{E} = a^*_{\text{PAR}} c_p \phi P_m \quad (13)$$

Therefore, the verification of a linear relationship between  $F$  and  $\alpha$  in natural samples at different times along the migratory cycle represents a simultaneous validation of the conditions established for using  $F$  to trace variations in  $c_p$ .

**Sampling:** Sediment samples were collected during low tide using plexiglass corers (1.9 cm internal diameter) on intertidal mudflats near Pancas salt marsh, located on the south margin of the Tagus estuary, Portugal. The sampling site has fine sediment (90% of particle sizes < 20  $\mu\text{m}$ ), colonised by microphytobenthic communities typically dominated by diatoms (Brotas & Plante-Cuny 1998), the genera *Navicula* and *Gyrosigma* being the most frequent at the sampling site (Serôdio et al. 1997). Sediment cores were collected on 5 to 6 d during each of 3 spring-neap tidal cycles, in July and November 1995, and March 1996. After collection, samples were taken to the laboratory (in Lisbon, about 20 km from the sampling sites) and immediately placed outside, in an artificial tidal system that simulated the immersion during high tide periods using estuarine water collected on the day of sediment sampling (Serôdio et al. 1997). Samples remained in the tidal system overnight, and all measurements were carried out in the laboratory, on the day after sample collection. Samples were carefully moved to avoid disturbances in the vertical structure of the sediment.

**$F_0$  and  $P$  versus  $E$  curves:**  $F_0$  and  $P$  versus  $E$  curve parameters were measured simultaneously on undisturbed microphytobenthos assemblages at different times along the migratory cycle, 3 to 5 times  $\text{d}^{-1}$ , covering the whole range of diurnal low and high tide situations over the spring-neap tidal cycle. A different core was used at each time of the day to avoid effects of removal on the migratory rhythm.  $F_0$  was measured by positioning the PAM fiberoptics (12 mm diameter) perpendicular to the sediment surface, at a fixed distance of 1 mm, as described by Serôdio et al. (1997).

The relative positions of the sample surface, the fiber-optics and the oxygen microelectrode were set with a micromanipulator to which the corer was attached.  $P$  versus  $E$  curves were constructed by exposing the same sediment core to 8 different incident irradiances. Under each irradiance, photosynthesis was measured at depth intervals of 50  $\mu\text{m}$  and then integrated over all depths. During high tides, photosynthesis was measured maintaining a ca 2 mm layer of water above the sediment surface. Because the distribution of photosynthetic biomass along light gradients may affect the shape of the  $P$  versus  $E$  curve independently of  $\alpha$  and  $P_m$  (Terasima & Saeki 1985, Leverenz 1988, Henley 1993),  $P$  versus  $E$  curves were fit to the model of Bannister (1979):

$$P(E) = \frac{\alpha P_m E}{[(P_m)^m + (\alpha E)^m]^{\frac{1}{m}}} \quad (14)$$

which includes a shape parameter  $m$  ( $1 \leq m < \infty$ ) that represents the convexity of the curve. The model was adjusted using a quasi-Newton estimation procedure, and only the curves for which the model explained >90% of total variance were considered for further analysis. To maximise the temporal resolution of the short-term variability associated with migratory rhythms, only 2 replicated  $P$  versus  $E$  curves, each typically taking about 30 min to complete, were constructed at each point in the migratory cycle. Chl  $a$  fluorescence was measured immediately before and after the construction of the  $P$  versus  $E$  curves, and the parameters estimated for each curve were compared with the adjoining  $F_0$  measurement.

## RESULTS

### $F$ versus $c$ : temperature and light effects

$F_0$  was the fluorescence parameter least sensitive to variations in temperature or irradiance (Figs 2 & 3). With the exception of *Spirulina maxima*,  $F_0$  varied less with temperature than all the other fluorescence parameters: 10.4% in *Phaeodactylum tricornutum* and 10.5% in *Euglena granulata*. Most of the 50.2% variation in  $F_0$  observed with *S. maxima* occurred below 10°C;  $F_0$  varied by only 12.3% over the temperature range of 10 to 35°C. The chl  $a$  fluorescence parameters measured under actinic light,  $F_s$  and  $F_m'$ , were generally much more affected by temperature than dark-adapted  $F_0$  or  $F_m$ , exhibiting complex and diverse response patterns in all species, particularly in *P. tricornutum* (Fig. 2). Exposure to high irradiance resulted in most cases in quenching of fluorescence emission, which was particularly evident under actinic light.  $F_s$

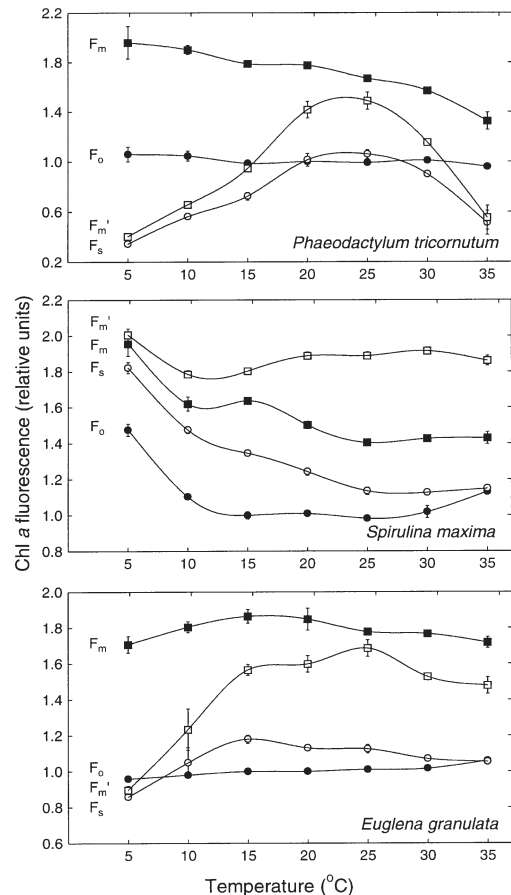


Fig. 2. Variation of chl  $a$  fluorescence parameters  $F_0$  (●),  $F_m$  (■),  $F_s$  (○) and  $F_m'$  (□) with temperature (actinic light: 200  $\mu\text{mol m}^{-2} \text{s}^{-1}$ ). Points represent the mean of 3 independent measurements, normalised to the value of  $F_0$  measured at growth temperature (20°C); error bars represent 1 standard deviation

and  $F_m'$  were the parameters most affected by the variation in incident irradiance in all species (Fig. 3). The quenching of fluorescence intensity was also observed in dark-adapted  $F_0$  and  $F_m$  over the range of irradiances tested, resulting in a maximum decrease of 45.9%, in *P. tricornutum*. Nevertheless,  $F_0$  was in all cases the least affected parameter by changes in incident irradiance.

### $f$ variability with $E$ and $c$

Both Eqs (10) & (11) described adequately the experimental data used for estimating the parameters of Eq. (9), thus validating the assumptions made for their derivation, namely the vertical homogeneity of the sediment deposits and the invariance of  $k_p$ ,  $k_F$ ,  $R$  and  $\mu$  with depth. The attenuation coefficients for downwelling photosynthetically absorbed irradiance and for fluorescence intensity were estimated as  $k_p = 16.85 \text{ mm}^{-1}$  [ $P(0)/E = 0.155 \text{ mmol O}_2 \text{ dm}^{-3} \text{ h}^{-1}$  ( $\mu\text{mol}$



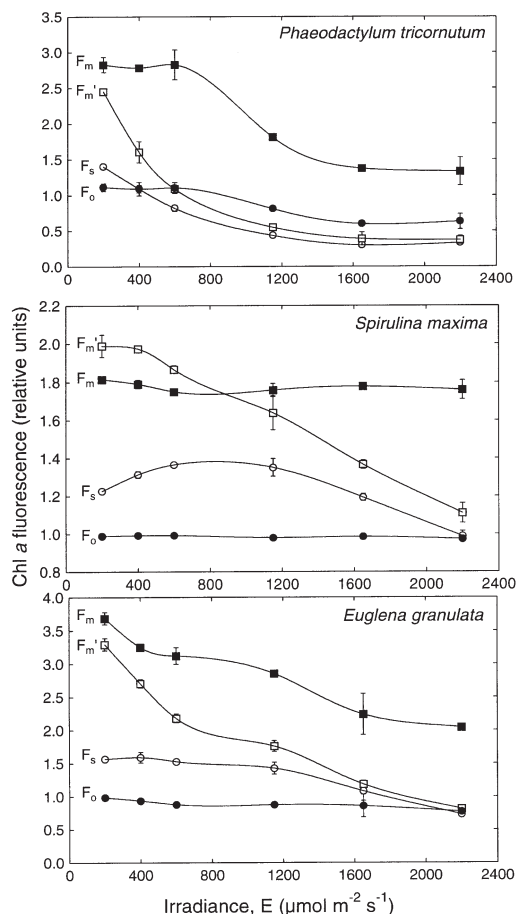


Fig. 3. Variation of chl *a* fluorescence parameters  $F_0$  (●),  $F_m$  (■),  $F_s$  (○) and  $F_m'$  (□) with irradiance.  $F_0$  and  $F_m$  were measured after 5 min of dark adaptation following exposure to indicated irradiance. Points represent the mean of 3 independent measurements, normalised to the value of  $F_0$  measured before light exposure; error bars represent 1 standard deviation

$\text{m}^{-2} \text{s}^{-1})^{-1}$ ;  $r = 0.934$ ,  $n = 39$ ) and  $k_F = 53.48 \text{ mm}^{-1}$  [ $F(0) = 8.884 \text{ V}$ ;  $r = 0.979$ ,  $n = 7$ ], respectively. The detection limits for the measurement of fluorescence intensity and rate of photosynthesis were determined to be  $L_P = 0.07 \text{ mmol O}_2 \text{ dm}^{-3} \text{ h}^{-1}$  and  $L_F = 0.002 \text{ V}$  (for the instrument settings used for measuring all the data presented). By applying these estimates to Eqs (7) & (8),  $z_P$  was calculated for the range of variation in  $E$ :  $z_P$  increases non-linearly with surface irradiance, exceeding  $z_F$  for most of the range of incident irradiance (Fig. 4A); under  $2000 \mu\text{mol m}^{-2} \text{ s}^{-1}$ , photosynthesis can be measured down to a depth of  $z_P = 0.5 \text{ mm}$ , while the fluorescence measured at

the surface corresponds to a depth interval of  $z_F = 0.16 \text{ mm}$  ( $z_P/z_F = 3.21$ ). By applying Eq. (6),  $f$  was found to remain virtually constant under most of the range of  $E$  and  $c$  values typically found *in situ*, approaching the value of  $k_P/k_F = 0.32$  (Fig. 4B). Largest variations in  $f$  take place when both  $E$  and  $c$  attain low values. For the extreme situation of  $c = 25 \text{ g chl a m}^{-3}$  (typical value before sunrise),  $f$  varies  $< 2\%$  between 40 and  $2000 \mu\text{mol m}^{-2} \text{ s}^{-1}$ .

### *f* variability *in situ*

Vertical profiles of  $\ln[P(z)/E]$  were consistently different between low and high tide situations. While a linear regression equation could be fitted to 77.8% of the profiles measured during low tide, this number was reduced to 47.6% during high tides. Of the non-linear profiles found during low tides, 83.3% were measured  $< 30 \text{ min}$  before high tide or  $< 1 \text{ h}$  before sunset, times in which the downward migration of microalgae is expected. Non-linearity of high tide profiles was often due to the presence of a production maximum clearly below the surface (Fig. 5A).

Changes in the chl *a* profile under *in situ* conditions were found to cause more variability in  $f$  than  $E$  or  $c$ .  $f$  variability was lower during daylight exposure periods (CV 17.2%) than during periods of inundation (CV 29.8%). The same pattern was also found for all sampling periods separately. During low tide,  $f$  variability was higher near high tide or night; when excluding from the analysis the first hour after or before inundation or night, variability (CV) decreased to 15.4%, and to 11.4% when the first 2 h are excluded.

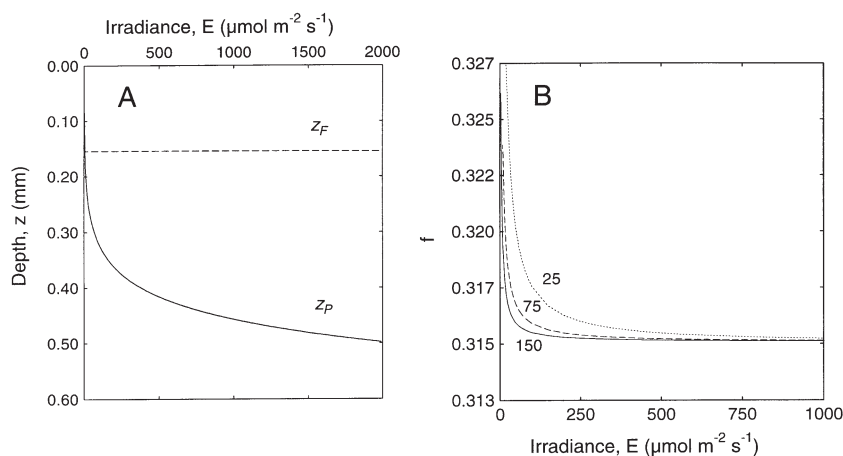


Fig. 4. Calculated variation of (A) depth interval contributing to depth-integrated dark-level chl *a* fluorescence detectable at the surface,  $z_F$ , and for measurable photosynthesis,  $z_P$ , and (B)  $f$ , the fraction of productive biomass detected by depth-integrated fluorescence, with surface irradiance, for different values of chl *a* concentration, homogeneously distributed over the photic zone (25, 75 and  $150 \text{ g chl a m}^{-3}$ )

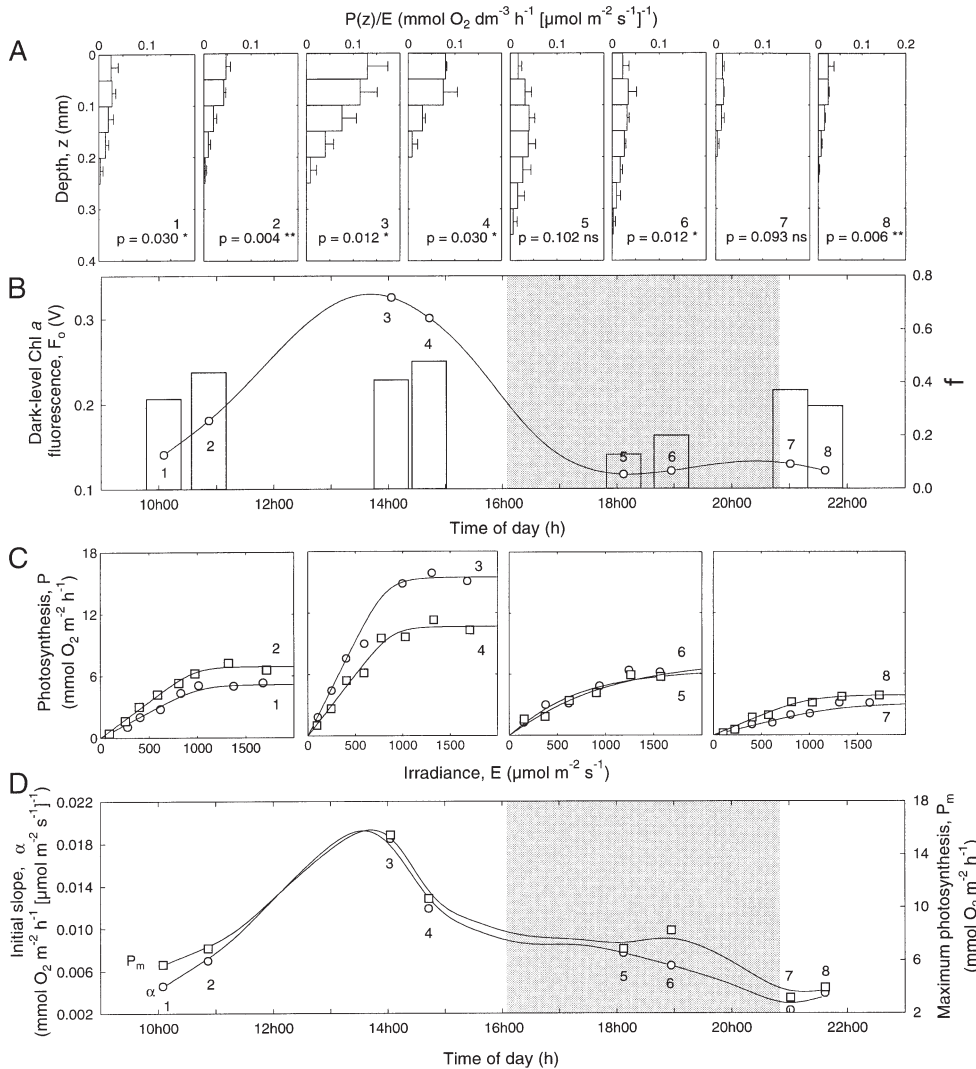


Fig. 5. Example of the effects of migratory rhythms on short-term variability of the photosynthetic light response of intact microphytobenthos communities under *in situ* conditions during 1 d. Hourly variation of (A) vertical profiles of  $P(z)/E$ , (B)  $F_0$  (line) and  $f$  (bars), (C) community-level  $P$  versus  $E$  curve, and (D)  $P$  versus  $E$  curve parameters  $\alpha$  and  $P_m$ . Shaded periods represent high tide. During the diurnal low tide, the vertical migration of the microalgae causes the variation of the total chl  $a$  concentration in the photic zone, while not significantly affecting the uniformity of its vertical distribution (A). In (A), the probability associated with the fitting of a linear regression equation to the vertical profile of  $\ln[P(z)/E]$  is indicated. Downward migration during high tide causes a marked change in the shape of the vertical profile of  $P(z)/E$ , now deeper and maximal below the surface; in the short period between ebb and sunset microalgae migrate downward, and a uniform distribution is found only in 1 of the 2 profiles (A). The hourly variation in productive biomass is closely followed by  $F_0$  as  $f$  remains relatively constant during low tide (B), and leads to substantial changes in the community photosynthetic light response  $P$  versus  $E$  curve (C,D). Both  $\alpha$  and  $P_m$  showed highly significant correlation with  $F_0$  ( $p < 0.001$ )

When considering single low tide periods, maximum variation in  $f$  ranged from 103 to 155%, with a mean value of 135%. Intraday variability in  $f$  is illustrated in Fig. 5B, which shows  $f$  remaining relatively constant during low tide periods, and decreasing most markedly during inundation.

#### Effects of varying productive biomass on photosynthetic light response

Both  $\alpha$  and  $P_m$  varied significantly during the course of daylight low tide periods, reaching maximum values during the middle of exposure periods and minimum values when approaching high tide or night.  $F_0$  exhibited consistently similar hourly patterns of variation, and significant correlations were found both between  $F_0$  and  $\alpha$  and between  $F_0$  and  $P_m$  for all spring-neap tidal cycles (Figs 6 & 7). As a consequence, highly sig-

nificant correlations were found between  $\alpha$  and  $P_m$  in all periods ( $p < 0.001$ ). The short-term variability in community-level  $P$  versus  $E$  curve parameters, paralleled by  $F_0$ , is illustrated in Fig. 5B to D. A clear difference was found between low and high tide periods: for low tide, a significant correlation was also found for all sampling periods, with  $F_0$  explaining from 57.5 to 81.8% of the variability observed in  $\alpha$ , and from 69.4 to 95.2% of the variability in  $P_m$ ; regarding high tide periods, a significant correlation was found only between  $F_0$  and  $\alpha$  in July ( $p = 0.014$ ,  $n = 8$ ). No significant correlation was found between  $F_0$  and  $m$ . No significant differences in the ratio  $F_0/\alpha$  (expected to be proportional to  $f$ ) were found between linear and non-linear profiles (2-sided  $t$ -test,  $p > 0.05$ ). This was verified when considering each sampling period separately, when pooling the data from the 3 sampling periods, or when considering low and high tides separately.

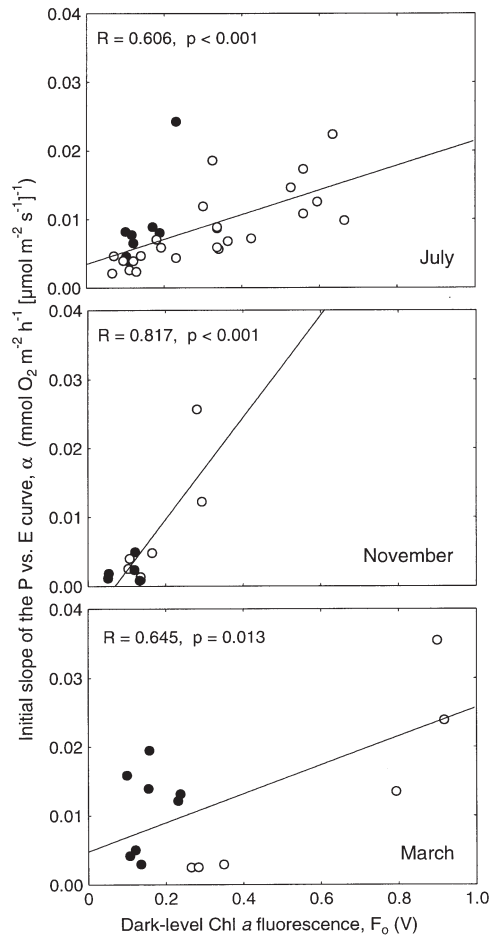


Fig. 6. Relationship between dark-level chl *a* fluorescence,  $F_0$ , and the initial slope of the depth-integrated  $P$  versus  $E$  curve,  $\alpha$ , in undisturbed microphytobenthos assemblages over 3 spring-neap tidal cycles (July, November, March) (o: low tide; ●: high tide)

## DISCUSSION

### Tracing changes in productive biomass

#### $F$ versus $c$

Effects of light and temperature on fluorescence emission per unit of chl *a* were minimal when fluorescence was measured at its minimum or dark level.  $F_0$  was the least variable of the measured fluorescence parameters under the tested range of variation of light and temperature, in spite of the considerable diversity in the response pattern of the different species, being confirmed as the most adequate fluorescence parameter to trace variations in chl *a* concentration. This variability in response patterns is associated with fundamental differences in the composition and organisation of the photosynthetic membranes and other characteristics affecting the func-

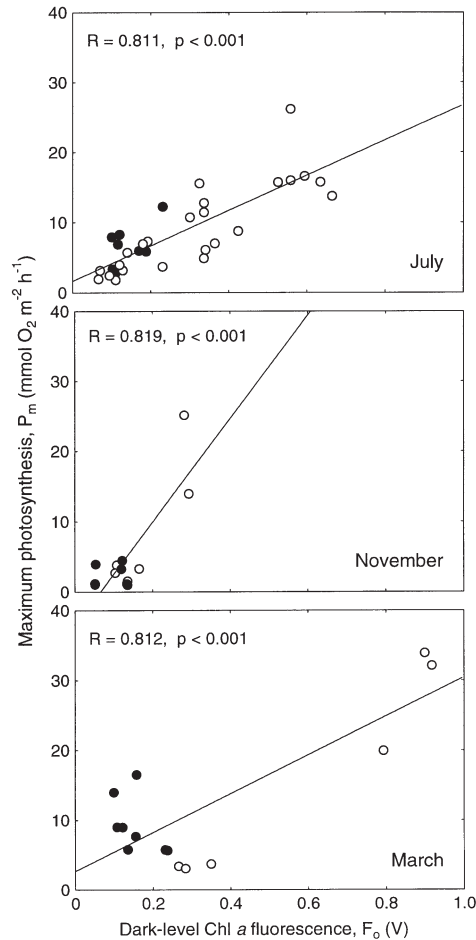


Fig. 7. Relationship between dark-level chl *a* fluorescence,  $F_0$ , and depth-integrated maximum photosynthesis,  $P_m$ , in undisturbed microphytobenthos assemblages over 3 spring-neap tidal cycles (July, November, March) (o: low tide; ●: high tide)

tioning of the photosynthetic apparatus, the discussion of which is beyond the scope of this study.  $F_0$  was also the least variable parameter when comparing between species, which is important for maintaining a low variability in the quantum yield of fluorescence of the whole community, where short-term variations in the taxonomic composition of the microphytobenthos exposed to measuring light may occur due to differential cell migration. Fluorescence parameters measured under actinic light,  $F_s$  and  $F_m'$ , were strongly affected by changes in temperature and irradiance and are thus clearly inadequate for tracing variations of biomass in microphytobenthos samples, particularly when considering the high variability in temperature and light that characterises the estuarine intertidal environment (Seródio & Catarino 1999). The alternative approach of measuring  $F_m$  does not avoid an identically large variability with temperature and irradiance.

Significant variations in  $F_0$  emission per unit chl  $a$  may still take place, caused either by changes in  $a^*_{650}$  or in  $\phi F$  (Eq. 4). However, such variability is restricted to extreme situations leading to the inactivation of functional reaction centres, such as extreme temperatures, photoinhibiting irradiances or anaerobiosis (Büchel & Wilhelm 1993, Ting & Owens 1993, 1994). In particular, changes in  $a^*_{650}$  may occur as a result of relatively slow photoadaptive processes affecting pigmentation and chloroplast morphology (e.g. 10 h for a 10% variation in  $a^*_{PAR}$ ; Berner et al. 1989), or, on shorter time scales, as a result of non-photochemical quenching and the establishment of a trans-thylakoidal proton gradient in the dark caused by chlororespiration (Caron et al. 1987, Ting & Owens 1993, Schreiber et al. 1995). Such processes lead to significant decreases in  $F_0$  per unit chl  $a$  in natural marine phytoplankton exposed to high irradiance levels, associated with decreases in  $a^*_{PAR}$  (Falkowski et al. 1994). However, it may be expected that these processes will not confound the detection of short-term variations in photosynthetic biomass of intertidal microphytobenthos under natural conditions, as the effects on  $F_0$  emission are much smaller than the typical variations in chl  $a$  concentration in the photic zone caused by migratory rhythms (Serôdio et al. 1997).

However, uncorrelated changes in  $F_0$  and the chl  $a$  actually intervening in measurable photosynthesis, which constitutes the community productive biomass, may occur due to changes in  $a^*_{PAR}$  (Eq. 7), following variations in the spectrum of available solar light with time of day, cloud cover, and water or sediment depth. Because PAM fluorometry is based on the induction of fluorescence emission through the application of a monochromatic light,  $F_0$  emission may not reflect variations in the spectral composition of the light in use by the photosynthetic apparatus, which has been the basis for the application of chl  $a$  fluorescence techniques to the quantification of the photosynthetic light absorption by marine phytoplankton (Sosik & Mitchell 1995) and the estimation of its biomass or primary production (Kiefer et al. 1989, Chamberlin et al. 1990). However, solar-induced ('passive') fluorescence, although reflecting the changes in the spectral characteristics of absorbed light by resulting from the absorption of the full solar light spectrum, has the disadvantage of being affected by the large short-term variability in  $\phi F$  associated to the response of the photosynthetic apparatus to changes in temperature or incident irradiance.

#### Depth-integration: $F$ versus $c_p$

When considering the depth-integration of fluorescence emission, the results indicate that only a fraction

of total  $c_p$  is detectable by  $F_0$ , as  $z_F$  remains smaller than  $z_p$  under most of the range of  $E$  and  $c$ . The value estimated for  $z_F$  (0.160 mm) is quite similar to that obtained by Kromkamp et al. (1998), 0.175 mm, in spite of being determined by a different experimental approach. The value estimated for  $k_p$ ,  $16.85 \text{ mm}^{-1}$ , is within the range of previous estimates, both for similar sediments of the Tagus estuary ( $17.29 \text{ mm}^{-1}$ , Serôdio et al. 1997) and as for the muddy sediments of other estuaries ( $32.6 \text{ mm}^{-1}$ , Colijn 1982;  $11.3$  to  $12.7 \text{ mm}^{-1}$ , Baillie 1987). The higher value of  $k_F$  ( $k_F/2 = 26.74 \text{ mm}^{-1}$ , the average value correspondent to only downwelling irradiance) relative to  $k_p$  is to be expected from the highest absorption in the red zone of the spectrum due to the presence of chl  $a$  and other photosynthetic pigments.

However, the detectable fraction of  $c_p$  can be expected to be sufficiently constant to allow for the use of  $F_0$  to proportionally follow variations in  $c_p$ . The detection limit for  $F_0$  was found to be sufficiently low to ensure that the variability resulting solely from changes in  $E$  or  $c$  may be considered as negligible or to occur during well-defined periods, when both  $E$  and  $c$  are low. Because *in situ*, low values of  $E$  and  $c$  occur simultaneously only shortly after dawn and before nightfall, variability in  $f$  may be expected to be minimal during most of daylight hours. Relevant variability in  $f$  may thus be assumed to result mostly from short-term changes in the chl  $a$  profile following migratory movements of microalgae. However, the analysis of the  $P(z)/E$  profiles indicated that, at least during diurnal low tide, the vertical distribution of chl  $a$  in the photic zone appears not to depart significantly from uniformity. Furthermore, the variability in  $f$  caused by changes in the vertical chl  $a$  profile under *in situ* conditions, quantified by calculating  $f$  for a wide range of chl  $a$  profiles, was found to be much smaller than the variability caused by fluctuations in total chl  $a$  present in the photic zone during single migratory cycles: in samples under *in situ* conditions, changes in  $F_0$  during single low tide exposure periods typically range from 400 to 900% (Serôdio et al. 1997), while the maximum difference found between  $f$  values calculated for the same day averaged 135%.

The finding of a relative uniformity in chl  $a$  profiles during vertical migrations may be explained by the small depth interval of the photic zone (maximum  $500 \mu\text{m}$ , under  $2000 \mu\text{mol m}^{-2} \text{ s}^{-1}$ ) in comparison with the depth interval where migrations cause variations in the chl  $a$  concentration (down to 3 mm; Pinckney et al. 1994). Because the maximum photic depth is about 10 times the length of the smaller diatoms and 2 to 3 times the length of the larger cells, large variations in  $F_0$  or production may be expected to result more from cells entering or leaving the photic zone than from changes

in their positioning within this zone. Moreover, because the fluorescence signal measured by the PAM fiberoptics integrates over an area of ca 1.13 cm<sup>2</sup> (10<sup>4</sup> times larger than the cross-section of an hypothetical spherical cell of 50 µm in diameter), it may be expected to attenuate the effect of local extreme profiles and approximate a uniform chl *a* profile.

While it may be assumed that *f* remains relatively constant during low tide, the results indicate that important variations can occur near the transition to periods of high tide or night. Such changes are probably associated with the downward movement of microalgae during the periods shortly preceding and following high tide or night, causing the *F*<sub>0</sub> signal to correspond to a smaller fraction of *c*<sub>p</sub>. In fact, *f* was found to be, on average, higher during low tide (*f* = 0.41) than during high tide (*f* = 0.21). However, the variability in the chl *a* profile appears not to be sufficiently high to substantially affect the relationship between *F*<sub>0</sub> and *c*<sub>p</sub>, as no significant differences were found between the value of the ratio *F*<sub>0</sub>/*α* calculated for linear and non-linear profiles.

The significant correlation found between *F*<sub>0</sub> and the *P* versus *E* curve parameter *α* over the range of *in situ* variability further confirms the ability to trace variations in *c*<sub>p</sub> using *F*<sub>0</sub>. Moreover, other factors besides the relationship between *F*<sub>0</sub> and *c*<sub>p</sub> are likely to confound the verification of a correlation between *F*<sub>0</sub> and *α*. First, the large difference between the scales of spatial (horizontal) variability resolved by the fluorometer fiberoptics and the microelectrode tip may have led to much of the observed data variability. Second, the variability in *a*<sup>\*</sup><sub>650</sub>/*a*<sup>\*</sup><sub>PAR</sub> or *φP* affecting the physiological light response of the community may have induced variations in *α* uncorrelated to *F*<sub>0</sub>.

### Normalisation of community-level photosynthetic rates

One of the main interests in defining and quantifying the productive biomass of microphytobenthic assemblages lies in the possibility to normalise community-level photosynthetic rates, as a way to characterise the photophysiological response of the community independently of migratory movements and other factors affecting the photosynthetic biomass in the photic zone. The common practice of estimating microphytobenthic productive biomass through quantification of the chl *a* content of the top layers of sediment results from the direct application of the methodology developed and routinely used for phytoplankton. However, in contrast with the water column, the quantification of the vertical distribution of the chl *a* within the photic zone of the sediment presents considerable difficulties,

and chl *a* is usually quantified for a single depth interval. Estimates of *P*<sup>B</sup> obtained in this way are largely arbitrary, since they depend on the sectioning depth used for chl *a* extraction (MacIntyre et al. 1996). Moreover, because the depth interval used for chl *a* extraction, 2 mm (Rasmussen et al. 1983, Pinckney & Zingmark 1991), 5 mm (Sundbäck 1986, Blanchard & Montagna 1992) or 10 mm (Grant 1986, Brotas & Catarino 1995), is much larger than the photic zone, most of the quantified chl *a* originates from layers never illuminated and not contributing to the measured photosynthesis. As a consequence, biomass-specific photosynthetic rates may be expected to be largely underestimated, which can be confirmed by the fact that published values of *α*<sup>B</sup> estimated by this procedure, 1.9 to 3.1 × 10<sup>-3</sup> (Pinckney & Zingmark 1993) or 2.1 × 10<sup>-3</sup> mg C mg<sup>-1</sup> chl *a* h<sup>-1</sup> (µmol m<sup>-2</sup> s<sup>-1</sup>)<sup>-1</sup> (Brotas & Catarino 1995), are typically 1 to 2 orders of magnitude lower than the values estimated using resuspended microphytobenthic cells, for which the quantified chl *a* approximates the amount actually contributing to the measured photosynthesis: 0.1 to 1.6 × 10<sup>-1</sup> (Blanchard & Montagna 1992), 1.3 to 2.8 × 10<sup>-2</sup> (Rasmussen et al. 1983) and 3.5 to 8.0 × 10<sup>-2</sup> mg C mg<sup>-1</sup> chl *a* h<sup>-1</sup> (µmol m<sup>-2</sup> s<sup>-1</sup>)<sup>-1</sup> (MacIntyre & Cullen 1995).

One particularly appealing aspect of using active chl *a* fluorometry to quantify microphytobenthic productive biomass lies in the fact that it uses a light beam as a measuring probe for the chl *a* present in the photic zone. Because the measuring light parallels the behaviour of natural light within the sediment, the measured fluorescent signal may be closely related to the integrated vertical distribution of chl *a*, weighted, at each depth, by its contribution to community photosynthesis. In principle, any chl *a* fluorometer applying a low intensity measuring light beam conducted through a fiberoptics bundle can be used to non-destructively quantify the productive biomass of intact microphytobenthos samples. However, modulated fluorometers are particularly suitable for this purpose, as the intensity of the measuring light may be reduced to a level that is low enough to allow accurate measurement of the *F*<sub>0</sub> level.

Considering the results obtained on the uniformity of the chl *a* vertical profile, on the range of variation of *z*<sub>p</sub>, and on the value of *k*<sub>p</sub>, the productive biomass of a microphytobenthic assemblage may be approximated by simplifying Eq. (3):

$$c_p \approx \frac{c}{k_p} (e^{-k_p z_p}) \approx \frac{c}{k_p} \quad (15)$$

where *c* may be estimated from a calibration curve established between fluorescence intensity, *F* (V), and the sediment chl *a* content, *c* (mg chl *a* m<sup>-3</sup>), of vertically homogeneous sediment deposits with varying

microalgal content (Serôdio et al. 1997). The value of  $k_p$  may be estimated from vertical profiles of light-limited photosynthesis, obtained in the measuring of  $P$  (Eq. 10). Alternatively, because  $k_p$  is mainly determined by sediment characteristics, and therefore relatively invariant in comparison to  $c$ , existing estimates for the same sediment type may be used.

The error associated with the quantification of  $c_p$  applying Eq. (15), resulting from assuming a homogeneous chl  $a$  vertical distribution, can be assessed by comparing the values of  $c_p$  obtained by applying Eqs (3) & (15) to the range of chl  $a$  profiles found *in situ* [using, as for the calculation of  $f$  (Eq. 12), profiles of  $P(z)/E$  as proxies for  $c(z)$ , and, for Eq. 15,  $c = c_F k_F$ ]. On average,  $c_p$  resulted in overestimation by a factor of 1.30 during low tide, and underestimation by a factor of 0.66 during high tide. Even considering individual profiles,  $c_p$  estimates were always within the order of magnitude of expected values, with maximum error attaining 78%. This level of error represents a significant improvement regarding the precision in the quantification of the biomass to be used in the normalisation of photosynthetic rates. The alternative way of calculating areal chl  $a$  concentration from the chl  $a$  present in the upper layers of the sediment yields  $P^B$  estimates that are underestimated by at least 2 orders of magnitude. This can be illustrated by a numerical example using typical values for the variables of Eq. (3), for the case of a uniform chl  $a$  profile ( $c = 10^5$  mg chl  $a$   $m^{-3}$ , the order of magnitude of the values obtained by measuring  $F_0$ ,  $k_p = 16.85$   $mm^{-1}$ , and maximum  $z_p = 0.50$  mm, correspondent to an incident irradiance level of 2000  $\mu mol$   $m^{-2}$   $s^{-1}$ ): while the productive biomass is  $c_p = 5.9$  mg chl  $a$   $m^{-2}$ , areal chl  $a$  concentration calculated from the top 2 mm section reaches  $2.0 \times 10^2$  mg chl  $a$   $m^{-2}$ . This difference may increase by 1 order of magnitude in the case of a sectioning depth of 10 mm and lower surface irradiance levels.

### Productive biomass and community-level efficiency of light absorption

In the characterisation of the photophysiological response of photosynthetic organisms through the construction of  $P$  versus  $E$  curves, it is usually implicit that the measured irradiance, generally incident irradiance, either approximates (in the case of diluted phytoplankton samples or microalgal cultures) or is proportional (in the case of leaves of macrophytes or higher plants) to the actual irradiance absorbed for photosynthesis. The  $P$  versus  $E$  curve parameters estimated in this way can be assumed to reflect only variations in the efficiency of conversion of absorbed light energy (quantum yield of photosynthesis), and be used to

characterise and compare the photophysiological response of identical samples over time or locations. In the case of undisturbed microphytobenthic assemblages,  $P$  versus  $E$  curves are usually based on the irradiance incident on the surface of the sediment (Grant 1986, Pinckney & Zingmark 1993, Brotas & Catarino 1995). The information thus gathered, while useful for the characterisation of the response of the community as a whole, describes an 'apparent' light response of the community, which is only partially determined by the 'inherent' photophysiological characteristics of the microalgal population. The characterisation of the photophysiological properties of the community, determined by the quantum yield of photosynthesis, requires the quantification not only of the chl  $a$  concentration, given by  $c_p$ , but also of the absorption cross-section of the microalgae present in the photic zone,  $a^*_{PAR}$  (Eq. 1). The joint vertical distribution of  $a^*_{PAR}$  and  $c$  along the light gradient within the photic zone defines the community-level efficiency of light absorption,  $\epsilon$ , a quantity representing the fraction of the light incident at the surface that is absorbed for photosynthesis by the whole microphytobenthic community:

$$\epsilon = \int_0^{z_p} a^*_{PAR}(z)c(z) \frac{R_{PAR}(z)}{\mu_{PAR}(z)} e^{-k_p z} dz \quad (16)$$

the quantification of which allows one to fully distinguish changes in light-harvesting efficiency (changes in  $a^*_{PAR}$  or  $c$ ) from variations in energy conversion efficiency (changes in  $\phi P$ ).

The viability of using  $F_0$  to trace variations in  $\epsilon$  depends on the variability of the ratio  $a^*_{650}/a^*_{PAR}$ , which, under natural conditions, may be affected by changes in  $a^*_{PAR}$  following variations in the spectrum of available solar light not detected in fluorescence emission induced by monochromatic light. However, the correlations found between  $F_0$  (depending on  $a^*_{650}$ ) and  $P$  versus  $E$  curve parameters (depending on  $a^*_{PAR}$ ) indicate that, at least within each fortnightly cycle, the variability in  $a^*_{650}/a^*_{PAR}$  is much lower than the variability in  $c_p$ . This suggests that the measurement of  $c_p$  alone may allow tracing of most of the variability in  $\epsilon$ , and distinguishing variations in light-harvesting efficiency from variations in energy conversion efficiency, as the cause for the short-term variability in microphytobenthic photosynthesis.

One application of these results is the possibility to use estimates of  $c_p$  to calculate absolute estimates of  $\epsilon$  and  $\phi P$  for undisturbed communities, providing that  $a^*_{PAR}$  is known. This can be illustrated considering the numerical example presented above ( $c_p = 5.9$  mg chl  $a$   $m^{-2}$ ): using a typical value of  $a^*_{PAR} = 0.0075$   $m^2$   $mg^{-1}$  chl  $a$  (Hartig et al. 1998), light absorption efficiency reaches  $\epsilon = 4.5\%$ , varying between ca 2 and 14% for the range of variation of  $F_0$  observed *in situ* ( $\epsilon =$

$a^*_{PARc_P}$ ; Eq. 16 for a uniform photic zone); community  $\phi P_m$  can be calculated by additionally considering the corresponding value of  $\alpha$  [Eq. 13;  $\alpha = 9.1 \times 10^{-3}$  mmol  $O_2$   $m^{-2} h^{-1}$  ( $\mu\text{mol } m^{-2} s^{-1})^{-1}$ , estimated from the linear relationship with  $F_0$ ], which results in  $\phi P_m = 0.057$  mol  $O_2$  mol quanta $^{-1}$ , a value which is within the range of values measured for phytoplankton under identical nutrient concentrations (ca 10  $\mu\text{M } NO_3^-$ ; Babin et al. 1996). It may be also noted that, by normalizing  $\alpha$  to  $c_P$ , the resulting estimates of  $\alpha^B$  are within the order of magnitude of estimates calculated from resuspended microphytobenthos: for the same example,  $\alpha^B = 1.8 \times 10^{-2}$  mg C  $mg^{-1}$  chl  $a$   $h^{-1}$  ( $\mu\text{mol } m^{-2} s^{-1})^{-1}$ .

### Microphytobenthic primary production periodicity: migratory rhythms versus physiology

Aquatic primary producers typically control their photosynthetic light response through changes in the efficiency of conversion of absorbed light. Light absorption is largely determined by light availability and controlled by external processes affecting either the position of the photosynthetic cell in the environmental light gradient (e.g. mixing of the water column, in the case of phytoplankton) or the optical properties of the medium (e.g. turbidity of the water column, in the case of subtidal phytobenthos). In the case of microphytobenthos growing on fine intertidal sediments, the comparable dimensions of the photic zone of the sediment and of the motile microalgae enables the movement of individual cells over the vertical light gradient to result in substantial variations in the efficiency of light absorption at the community level. In this way, microphytobenthos communities have the ability to control their photosynthetic light response not only through changes in the photosynthetic yield at the level of the photosynthetic apparatus of individual cells, but also by actively regulating the fraction of available light that is absorbed for photosynthesis.

The results of this study indicate that the effects of migratory rhythms in regulating the community photosynthetic response are actually more important than those resulting from photophysiological adaptation, therefore identifying microalgal migratory behaviour as the main factor controlling short-term variability in the community light utilisation efficiency. The finding of significant correlations between  $P$  versus  $E$  curve parameters and  $F_0$  in all sampling periods indicates that, at least on hourly to fortnightly time scales, a significant proportion of the variability in the photosynthetic light response of the studied communities is explained solely by variations in the efficiency of light absorption, and not by variations in the efficiency of light energy conversion. Although short-term varia-

tions in photosynthetic efficiency of microphytobenthos have been reported (Blanchard & Cariou-Le Gall 1994, Kromkamp et al. 1998), the assessment of their relative effect on the variability of community photosynthesis has been limited by the impossibility of quantifying the effects of changes in light absorption efficiency associated with variations in productive biomass. Nevertheless, the existing evidence seems to confirm the findings of the present study, as the variability in biomass-independent photosynthetic light response observed in other studies is much lower than the variability in productive biomass reported here. While hourly variations in productive biomass may reach values near to 1 order of magnitude, maximum reported values for hourly variability in  $\alpha^B$  or  $P_m^B$ , measured in resuspended samples, attain only ca 81.8 and 90.6%, respectively (Blanchard & Cariou-Le Gall 1994). Moreover, much lower variability was measured in the photosynthetic efficiency of undisturbed microphytobenthic communities under *in situ* conditions (Kromkamp et al. 1998). The significant difference found among the slopes of the regression lines, both for the  $\alpha$  versus  $F_0$  and for the  $P_m$  versus  $F_0$  plots, in spite of resulting from a small number of extreme observations (November, Figs 6 & 7), suggests the occurrence of variations in physiological parameters that can alter the quantitative relationship between  $F_0$  and  $c_P$ . Seasonal variations in  $\phi F_0$  may result from changes in thylakoid stacking and membrane transparency ('package effect') or pigmentation (Berner et al. 1989), nutrient depletion (Geider et al. 1993), or be associated with changes in taxonomic composition, which could affect PSII:PSI stoichiometry or relative absorption cross section (Caron et al. 1987, Büchel & Wilhelm 1993).

It has been suggested that motile benthic microalgae use their migratory ability to actively search for optimal light levels for photosynthesis within the photic zone, thus maximising light absorption while avoiding exposure to photoinhibiting light levels (Admiraal 1984). It may be hypothesised that such behaviour represents a rapid, flexible and energetically cheap way to optimise photosynthesis, reducing the need to undergo photophysiological adaptations at the level of the photosynthetic apparatus, and therefore explaining the low variability observed in the photophysiological light response of the microphytobenthos.

This study showed that the measurement of  $F_0$  on undisturbed microphytobenthic assemblages allows quantitative assessment of the effect of the migratory rhythms on the temporal variability of microphytobenthic primary productivity, and distinction of variations in light-harvesting efficiency from variations in energy conversion efficiency as the cause for the short-term variability in community-level photosynthesis. The presented results further highlight the ecological impor-

tance of the definition and quantification of the productive biomass of intertidal microphytobenthic communities. For the studied microphytobenthos of the Tagus estuary, the above was seen to represent the main source of short-term variability in the community photosynthesis and, consequently, in the first rate-limiting step of estuarine benthic primary productivity. The application of the technique to other estuarine ecosystems or habitats would assess the extent to which the periodicity often observed in intertidal microphytobenthic primary production results from migratory rhythmicity.

**Acknowledgements.** The authors thank Dr Margarida Ramos for help with oxygen microelectrode instrumentation, and Paulo Cartaxana, Teresa Cabrita and Ana Amorim-Ferreira for help with the field and laboratory work. Dr Lília Santos kindly provided the *Euglena granulata* culture. This work was supported by Junta Nacional de Investigação Científica e Tecnológica, Grants PFMRH 359/92 and PRAXIS XXI BD/5045/95 to João Serôdio. We thank Drs Ulrich Schreiber and Vanda Brotas, and 4 anonymous reviewers for critical comments on the manuscript. This work is a contribution to the European Union ELOISE Programme (ELOISE No. 102) and was carried out under the framework of the Marine and Science and Technology Programme (MAST III) under the NICE Project Contract MAS3-CT96-0048, and EUROSSAM Project Contract ENV4-CT97-0436.

#### LITERATURE CITED

- Admiraal W (1984) The ecology of estuarine-inhabiting diatoms. *Prog Phycol Res* 3:269–322
- Babin M, Morel A, Claustre H, Bricaud A, Kolber Z, Falkowski PG (1996) Nitrogen- and irradiance-dependent variations of the maximum quantum yield of carbon fixation in eutrophic, mesotrophic and oligotrophic marine systems. *Deep-Sea Res* 43:1241–1272
- Baillie P (1987) Diatom size distribution and community stratification in estuarine intertidal sediments. *Estuar Coast Shelf Sci* 25:193–209
- Bannister TT (1979) Quantitative description of steady state, nutrient-saturated algal growth, including adaptation. *Limnol Oceanogr* 24:76–96
- Berner T, Dubinsky Z, Wyman K, Falkowski PG (1989) Photoadaptation and the 'package' effect in *Dunaliella tertiolecta* (Chlorophyceae). *J Phycol* 25:70–78
- Blanchard GF, Cariou-Le Gall V (1994) Photosynthetic characteristics of microphytobenthos in Marennes-Oléron Bay, France: preliminary results. *J Exp Mar Biol Ecol* 182:1–14
- Blanchard GF, Montagna PA (1992) Photosynthetic response of natural assemblages of marine benthic microalgae to short- and long-term variations of incident irradiance in Baffin Bay, Texas. *J Phycol* 28:7–14
- Brotas V, Catarino F (1995) Microphytobenthos primary production of the Tagus estuary (Portugal). *Neth J Aquat Res* 29:333–339
- Brotas V, Plante-Cuny MR (1998) Spatial and temporal patterns of microphytobenthic taxa of estuarine tidal flats in the Tagus Estuary (Portugal) using pigment analysis by HPLC. *Mar Ecol Prog Ser* 171:43–57
- Büchel C, Wilhelm C (1993) *In vivo* analysis of slow chlorophyll fluorescence induction kinetics in algae: progress, problems and perspectives. *Photochem Photobiol* 58:137–148
- Caron L, Berkaloff C, Duval JC, Jupin H (1987) Chlorophyll fluorescence transients from the diatom *Phaeodactylum tricorutum*: relative rates of cyclic phosphorylation and chlororespiration. *Photosynth Res* 11:131–139
- Chamberlin WS, Booth CR, Kiefer DA, Morrow JH, Murphy RC (1990) Evidence for a simple relationship between natural fluorescence, photosynthesis and chlorophyll in the sea. *Deep-Sea Res* 37:951–973
- Colijn F (1982) Light absorption in the waters of the Ems-Dollard estuary and its consequences for the growth of phytoplankton and microphytobenthos. *Neth J Sea Res* 15:196–216
- Dubinsky Z, Berman T, Schanz F (1984) Field experiments for *in situ* measurement of photosynthetic efficiency and quantum yield. *J Plankton Res* 6:339–349
- Falkowski P, Kiefer DA (1985) Chlorophyll a fluorescence in phytoplankton: relationship to photosynthesis and biomass. *J Plankton Res* 7:715–731
- Falkowski PG, Green R, Kolber Z (1994) Light utilization and photoinhibition of photosynthesis in marine phytoplankton. In: Baker NR, Bowes J (eds) *Photoinhibition of photosynthesis: from molecular mechanisms to the field*. BIOS Scientific, Oxford, p 407–432
- Geider RJ, La Roche J, Greene RM, Olaizola M (1993) Response of the photosynthetic apparatus of *Phaeodactylum tricorutum* (Bacillariophyceae) to nitrate, phosphate, or iron starvation. *J Phycol* 29:755–766
- Grant J (1986) Sensitivity of benthic community respiration and primary production to changes in temperature and light. *Mar Biol* 90:299–306
- Hartig P, Wolfstein K, Lippemeier S, Colijn F (1998) Photosynthetic activity of natural microphytobenthos populations measured by fluorescence (PAM) and <sup>14</sup>C-tracer methods: a comparison. *Mar Ecol Prog Ser* 166:53–62
- Henley WJ (1993) Measurement and interpretation of photosynthetic light-response curves in algae in the context of photoinhibition and diel changes. *J Phycol* 29:729–739
- Kiefer DA, Chamberlin WS, Booth CR (1989) Natural fluorescence of chlorophyll a: relationship to photosynthesis and chlorophyll concentration in the western South Pacific gyre. *Limnol Oceanogr* 34:868–881
- Kolber Z, Falkowski PG (1993) Use of active fluorescence to estimate phytoplankton photosynthesis *in situ*. *Limnol Oceanogr* 38:1646–1665
- Krause GH, Weis E (1991) Chlorophyll fluorescence and photosynthesis: the basics. *Annu Rev Plant Physiol Plant Mol Biol* 42:313–349
- Kromkamp J, Barranguet C, Peene J (1998) Determination of microphytobenthos PSII quantum efficiency and photosynthetic activity by means of variable chlorophyll fluorescence. *Mar Ecol Prog Ser* 162:45–55
- Kühl M, Jørgensen BB (1994) The light field of microbenthic communities: radiance distribution and microscale optics of sandy coastal sediments. *Limnol Oceanogr* 39:1368–1398
- Leverenz JW (1988) The effects of illumination sequence, CO<sub>2</sub> concentration, temperature and acclimation on the convexity of the photosynthetic light response curve. *Physiol Plant* 74:332–341
- MacIntyre HL, Cullen JJ (1995) Fine-scale vertical resolution of chlorophyll and photosynthetic parameters in shallow-water benthos. *Mar Ecol Prog Ser* 122:227–237
- MacIntyre HL, Geider RJ, Miller DC (1996) Microphytobenthos: the ecological role of the 'secret garden' of unvegetated, shallow-water marine habitats. I. Distribution, abundance and primary production. *Estuaries* 19:186–201



- Morel A (1978) Available, usable, and stored radiant energy in relation to marine photosynthesis. *Deep-Sea Res* 25:673–688
- Paterson DM (1986) The migratory behaviour of diatom assemblages in a laboratory tidal micro-ecosystem examined by low temperature scanning electron microscopy. *Diatom Res* 1:227–239
- Pinckney J, Zingmark RG (1991) Effects of tidal stage and sun angles on intertidal benthic microalgal productivity. *Mar Ecol Prog Ser* 76:81–89
- Pinckney J, Zingmark RG (1993) Photophysiological responses of intertidal benthic microalgal communities to *in situ* light environments: methodological considerations. *Limnol Oceanogr* 38:1373–1383
- Pinckney J, Piceno Y, Lovell CR (1994) Short-term changes in the vertical distribution of benthic microalgal biomass in intertidal muddy sediments. *Diatom Res* 9:33–42
- Rasmussen MB, Henriksen K, Jensen A (1983) Possible causes of temporal fluctuations in primary production of the Danish Wadden Sea. *Mar Biol* 73:109–114
- Revsbech NP, Jørgensen BB (1983) Photosynthesis of benthic microflora measured with high spatial resolution by the oxygen microprofile method: capabilities and limitations of the method. *Limnol Oceanogr* 28:749–756
- Round FE, Palmer JD (1966) Persistent, vertical-migration rhythms in benthic microflora. II. Field and laboratory studies on diatoms from the banks of the river Avon. *J Mar Biol Assoc UK* 46:191–214
- Schreiber U, Bilger W (1987) Rapid assessment of stress effects on plant leaves by chlorophyll fluorescence measurements. In: Tenhunen JD, Catarino FM, Lange OL, Oechel WD (eds) *Plant response to stress*, Springer-Verlag, Heidelberg, p 27–53
- Schreiber U, Schliwa U, Bilger W (1986) Continuous recording of photochemical and non-photochemical chlorophyll fluorescence quenching with new type of modulation fluorometer. *Photosynth Res* 10:51–62
- Schreiber U, Endo T, Mi HL, Asada K (1995) Quenching analysis of chlorophyll fluorescence by saturation pulse method: particular aspects relating to the study of eukaryotic algae and cyanobacteria. *Plant Cell Physiol* 36:873–882
- Seródio J, Catarino F (1999) Fortnightly light and temperature variability in estuarine intertidal sediments and implications for microphytobenthos primary productivity. *Aquat Ecol* 33:235–241
- Seródio J, Marques da Silva J, Catarino F (1997) Nondestructive tracing of migratory rhythms of intertidal benthic microalgae using *in vivo* chlorophyll *a* fluorescence. *J Phycol* 33:542–553
- Sosik HM, Mitchell BG (1995) Light absorption by phytoplankton, photosynthesis pigments and detritus in the California Current System. *Deep-Sea Res* 42:1717–1748
- Sundbäck K (1986) What are the benthic microalgae doing on the bottom of Laholm Bay? *Ophelia* 4:273–286
- Terashima I, Saeki T (1985) A new model for leaf photosynthesis incorporating the gradients of light environment and of photosynthetic properties of chloroplasts within a leaf. *Ann Bot* 56:489–499
- Ting CS, Owens TG (1993) Photochemical and nonphotochemical fluorescence quenching processes in the diatom *Phaeodactylum tricorutum*. *Plant Physiol (Rockv)* 101:1323–1330
- Ting CS, Owens TG (1994) The effect of excessive irradiance on photosynthesis in the marine diatom *Phaeodactylum tricorutum*. *Plant Physiol (Rockv)* 106:763–770

*Editorial responsibility: Otto Kinne (Editor), Oldendorf/Luhe, Germany*

*Submitted: February 2, 2000; Accepted: October 31, 2000  
Proofs received from author(s): July 16, 2001*